Reviewer Comments

Jennifer Annoni

We would like to thank the reviewers and editor for the time that they spent examining our manuscript. Detailed responses to all the reviewer comments are provided below. We believe the manuscript has been greatly improved by addressing the reviewer comments.

1 Reviewer 1

This is an interesting paper, which compares several wake models to LIDAR measurements. The measurements are performed at a distance of 2.35D downstream of the turbine, and consider varying turbulence intensity and yaw angle. I believe that this paper is suitable for publication in WES, provided the authors address the minor comments below:

1. Page 1, abstract: It would be useful for the abstract to specify that the wake models are compared to the LIDAR data at a downstream distance of x = 2.35D.

   A reference to the distance downstream is now mentioned in the abstract.

2. Page 2, last line: there seems to be an unnecessary parenthesis before 'Bastankhah...'

   The parentheses were removed.

3. Page 4, limitations of the Jensen model: The authors should mention that, as noted by Frandsen et al. (Wind Energy 2006; 9:39-53), the Jensen model does not conserve momentum.

   This distinction has now been included in the limitations of the Jensen model and a reference to the Frandsen model is included.

4. Page 4, wake models: is there a reason to not consider the model introduced by Frandsen et. al., which does conserve momentum? It appears that the "gaussian model" discussed here might reasonably be considered a generalization of the 'Frandsen' model. It would be interesting to test this model as well, as it might provide a way of discerning the effects of conserving momentum versus using a gaussian profile.

   The authors agree that it would be interesting to include the Frandsen model, but in the interest of time and space, the Jensen, multi-zone, and Gaussian models were chosen. In addition, the three models chosen in this study were chosen based on their integration of wind farm controls. Each of the addressed models have been used in the context of wake steering. The authors may work to add the Frandsen model with a deflection model to future additions to the FLORIS model as another point of comparison.

5. Page 5, limitations of the multizone model: are the parameters in the model constrained in a manner ensuring that the wake model conserves momentum overall?

   No, momentum is not explicitly conserved. This point is now mentioned in the paper.

6. Page 5, Gaussian model, before equation (6): '...is computed using a Gaussian wake based on self-similarity theory often used in free shear flows, (Pope 2000).' A minor clarification - note that the solution shown for example in Pope (2000) is proven (not assumed) to be gaussian,

based on the assumption of self-similarity. Perhaps a slight re-wording to clarify this would be '... is computed by assuming a Gaussian wake, which is inspired by self-similarity theory often used in free shear flows, (Pope 2000).'

The wording has been changed as the reviewer suggested.

7. Page 6, equation (9): It's not clear how this is incorporated into the model - should this affect the leading term on the right-hand side of equation (10)?

   Equation 9 is the initialized flow field, which includes shear. The authors acknowledge the confusion and have updated equation 9 and 10 to indicate where the initial flow is incorporated. It now reads:

$$\frac{U_{init}}{U_\infty} = \left(\frac{z}{z_{hub}}\right)^{\alpha_s} \tag{1}$$

$$\frac{u(x,y,z)}{U_{init}} = 1 - Ce^{-(a(y-\delta)^2 - 2b(y-\delta)(z-z_{hub}) + c(z-z_{hub})^2)} \tag{2}$$

8. Page 7, capabilities and limitations of the gaussian model: the authors should mention here that this model conserves momentum.

   The authors include a note indicating that this model conserves momentum.

9. Page 13, Para. 2: the models are tuned to a subset of the data with low turbulence. What are the values of the coefficients?

   The following coefficients were used in this paper after being tuned and are also stated in the paper:

   - Jensen
     - $k_e = 0.055$
     - $k_d = 0.17$
   - Multi-zone
     - $k_e = 0.1$
     - $k_d = 0.17$
     - $m_e = -0.5, 0.3, 1.0$
     - $M_U = 0.47, 1.28, 5.5$
     - $a_U = 11.7$
     - $b_U = 0.72$
   - Gaussian
     - $k_a = 0.17$
     - $k_b = 0.06$

10. Section 4: All LIDAR data are collected quite close to the turbine, just 2.35D downstream, whereas turbines are usually separated by far larger distances. Could the authors briefly explain the value of this comparison (perhaps in the light of testing yaw models, since yaw effects are immediately discernible in the near wake)?

    The authors acknowledge that the limitations of this field test is that the wake is measured close to the turbine. However, the authors would like to emphasize that after tuning the models to the near wake, the models are able to perform reasonably well under varying atmospheric conditions and varying turbine operations even at close proximities. In addition, as the reviewer

indicates, this field test shows that wake steering can be seen at close ranges (Fleming et. al. 2017). Some work has been done to show that turbine wakes are only controllable within the first few diameters of the turbine (Raach et. al. 2016, Singh et. al. 2016). After that, the turbines become harder to control and should be described in a statistical sense.

11. Page 14, first line: the Jensen and multizone models are said not to have turbulence intensity as an input. Could the authors nevertheless please report what values of the fitting parameters would be required to get a good agreement? This would be helpful for any researchers who might wish to apply the Jensen/multi-zone models in high turbulence conditions.

    The authors were able to fit the Jensen model using a value of $k_e = 0.1$ for high turbulent scenarios ($TI > 10\%$) and multizone wake model using a value of $k_e = 0.13$. The author has noted this in the Appendix section.

12. Are there plans to make the data from this LIDAR campaign available, in some form, through an online repository?

    The data is still being processed with plans to release it to the public at a future date.

2 Reviewer 2

The manuscript presents the so-called FLORIS computational platform developed for quick optimization computations related to wind farm flow dynamics and power output. Specifically, the authors develop a comparison of wake velocity deficit between the several wake models in FLORIS with Lidar data. This reviewer considers that it is important that the community and also industry get to know about FLORIS, and its potential advantages and short-comes. It is for this reason that I believe that this is an interesting manuscript, well written that should be published. However, before publication I would encourage the authors to consider revisiting a few 'minor' items, just with the goal to improve clarity and completeness. The most relevant issues are referenced below. Please, also note that as a part of the review I introduce a commented PDF file, with a few suggestions to the wording of the document.

1. I had the impression that the abstract is hard to read and make a poor service to the manuscript. It wasn't until I actually read the manuscript that I understood what I was intending to read at the beginning. So please, consider clarifying the goal of the manuscript in the abstract section.

    The abstract has been updated to include a more clear and concise message. Below is the new abstract:

    The objective of this paper is to compare field data from a scanning lidar mounted on a turbine looking downstream at the turbine wake to controls-oriented wind turbine wake models. The measurements from the field campaign are used to validate controls-oriented tools used for wind plant controls and optimization. The National Wind Technology Center in Golden, CO conducted a demonstration of wake steering on a utility-scale turbine. In this campaign, the turbine was operated at various yaw misalignment set points while a lidar mounted on the nacelle scanned five downstream distances. Primarily, this paper examines measurements taken at 2.35 diameters downstream of the turbine. The lidar measurements were combined with turbine data, as well as measurements of the inflow made by a highly instrumented meteorological mast on-site. This paper presents a quantitative analysis of the lidar data as compared to the controls-oriented wake models used under different atmospheric conditions and turbine operation. These results show good agreement is obtained between the lidar data nd the models under these different conditions.

2. I did not really understand what was the reason or the use of the Lidar model in the actual manuscript. The comparisons done at the end of the manuscript are with respect to experimental data, isn't it?

   The lidar module was used to make sure that the 'measurements' taken from FLORIS could be compared one-to-one with the measurements in the field. Because the scanning lidar has a weighted function, some of the points are in the wake and some are outside of the wake. This provides a conservative estimate of the wake and the authors wanted to be sure this was not a source of discrepancy between the models and the data. The authors acknowledge that this point was not well documented in the current version of the paper and has been updated based on the reviewer's comments. The text added is indicated below:

   In particular, the scanning lidar used in the field campaign takes a weighted average of nine points along the line-of-sight trajectory. A lidar model is necessary to ensure this direct comparison. If any of the nine points are outside of the wake, the weighted average may lead to a more conservative estimate of the flow in the wake.

3. Could you clarify the last sentence in page 12 related to the periods of data used?

   The authors added a few sentences to make clear which periods of data were used in this analysis:

   In particular, the instruments on the met tower that are used to measure wind speed and direction are more reliable when they are not operating in the wake of nearby turbines or in the wake of its own tower due to blockage effects. We also chose to only include data where the turbine is operating normally. In this case, we define that as producing more than 100 kW. The turbine operation affects the wake properties and we need to ensure that we are comparing times when the turbine is performing as expected. Similarly, we only include times when the turbine yaw controller is tracking the specified offset within a few degrees to make a direct comparison with models.

4. In Figure 3 and in later figures where the lidar data is presented, it seems that for each sub-figure, corresponding to different level of turbulence intensity, a different number of scans used. Could the authors explain better the relationship between the number of scans and the quality of data? Phrased differently; does the number of scans affect your results? Is the number of scans related to the availability of data, and hence it is indicated as reference for the statistical analysis of the results? Or is it related to the number of scans necessary to get a good image, dependent on turbulence conditions, and hence presence of aerosols? If the number of scans does not affect the result, maybe then the authors should present results with the same number of scans for all cases, to eliminate a free parameter? In case this was done, is there other information that would be lost that I am not aware, or missing?

   Figure 3 demonstrates the differences in the flow based on the turbulence intensity. As the reviewer indicated, the number of scans affects the quality of the data represented in Figure 3. Due to the variability of this field test, the authors chose to use the most scans as possible to gain an understanding of the general trend of the data. The authors also saw the same general trends with the smallest number of scans; however, with fewer scans, the results are more uncertain. As a result, the authors chose to keep Figure 3 as is with additional explanation in the text:

   It is important to note that each image was generated with the maximum number of scans available after processing the data. More scans lead to a more robust measurement of the wake. A statistical analysis is presented in Figure 4, which indicates the effects of the limited number of scans processed.

5. At the end of the results section, could the authors argue a bit more on why the Jensen and multi-zone models work better under 'medium' turbulence intensity in yawed-conditions (Figure 6b) than in straight wake (Figure 6a)?

   The authors note this is odd and could potentially be explained by the way the yaw angle modifies the thrust generated by the turbine:

   In this case, the Jensen and multi-zone wake models have better agreement under yawed conditions than under normal conditions. One potential reason for this is that the "depth" of the wake is modified by the changing yaw angle, i.e. the thrust generated by the turbine is modified. This modified thrust is able to accommodate the under predictions in the normal operating case.

6. Please extend the discussion in the conclusions section. After making the effort of reading the manuscript, a reader would expect a more elaborated discussion/conclusion about the different wake models in FLORIS, as well as about FLORIS in general and its use for wind farm design and optimization.

   The authors have updated the discussion and conclusions sections to include a more thorough discussion of the results presented in the paper:

   This paper compared field data from a scanning lidar measuring the wake of a turbine in normal operating conditions and yaw misaligned conditions with controls-oriented models. Validating these controls models with field data in a variety of conditions is a critical step to implementing wind farm controls in the field. A quantitative analysis was done comparing the models in the FLORIS framework to this data. The data was processed to look at the effects of varying turbulence intensity levels as well as different yaw misaligned conditions. The wake models used in the comparison included the Jensen model, the multi-zone model, and the Gaussian wake mode. Future work will incorporate additional wake models that may be used in the context of wind farm controls. The Gaussian model provided the best representation of wake characteristics under different atmospheric conditions and different turbine operating conditions. Good agreement was also seen with the Jensen and multi-zone wake models on a smaller subset of data that matched the conditions of the tuning data.

   Based on these results, this provides more confidence in wind farm controllers designed using these models. This study provided a first step towards validating these models in the field. In particular, this study focused on the wake of a single turbine. An increased understanding of these models at the wind farm level is needed to determine the potential performance of wind farm controls solutions in the field.

Analysis of Control-Oriented Wake Modeling Tools Using Lidar Field Results

Jennifer Annoni[1], Paul Fleming[1], Andrew Scholbrock[1], Jason Roadman[1], Scott Dana[1], Christiane Adcock[1], Fernando Porte-Agel[2], Steffen Raach[3], Florian Haizmann[3], and David Schlipf[3]

[1]National Wind Technology Center, National Renewable Energy Laboratory, Golden, CO, 80401, USA
[2]Stuttgart Wind Energy (SWE), University of Stuttgart, Allmandring 5B, 70569 Stuttgart, Germany

Correspondence to: Jennifer Annoni (jennifer.annoni@nrel.gov)

Abstract.

~~Wind turbines in a wind farm operate individually to maximize their own performance regardless of the impact of aerodynamic interactions on neighboring turbines. Wind farm controls can be used to increase power production or reduce overall structural loads by properly coordinating turbines. One wind farm control strategy that is addressed in literature is known as wake steering, wherein upstream turbines operate in yaw misaligned conditions to redirect their wakes away from downstream turbines. The National Renewable Energy Laboratory (NREL)~~

The objective of this paper is to compare field data from a scanning lidar mounted on a turbine to controls-oriented wind turbine wake models. The measurements were taken from the turbine nacelle looking downstream at the turbine wake. This field campaign was used to validate controls-oriented tools used for wind plant controls and optimization. The National Wind Technology Center in Golden, CO conducted a demonstration of wake steering on a ~~single~~ utility-scale turbine. In this campaign, the turbine was operated at various yaw misalignment ~~setpoints~~ set points while a lidar mounted on the nacelle scanned five downstream distances. Primarily, this paper examines measurements taken at 2.35 diameters downstream of the turbine. The lidar measurements were combined with turbine data, as well as measurements of the inflow made by a highly instrumented meteorological mast ~~upstream. The full-scale measurements are used to validate controls-oriented tools, including wind turbine wake models, used for wind farm controls and optimization.~~ on-site. This paper presents a quantitative ~~comparison~~ analysis of the lidar data ~~and~~ as compared to the controls-oriented wake models used under different atmospheric conditions and turbine operation. ~~The~~ These results show good agreement is obtained between the lidar data ~~and~~ nd the models under these different conditions.

1 Introduction

~~Control strategies~~ Wind plant control can be used to maximize power production of a wind ~~farm~~plant, reduce structural loads to increase the lifetime of ~~turbines~~ turbine in a wind ~~farm~~plant, and better integrate wind energy into the energy market (Johnson and Thomas (2009); Boersma et al. (2017)). Typically, wind turbines in a wind ~~farm~~ plant operate individually to maximize their own performance regardless of the impact of aerodynamic interactions on neighboring turbines. ~~As a result, there~~ There

is the potential to increase power and reduce overall structural loads by properly coordinating turbine control actions. Two common wind ~~farm~~ plant control strategies in literature include wake steering and axial induction control. There has been a significant amount work done on wake steering~~in simulation~~, showing that this method has the most potential to increase power production (~~Gebraad et al. (2016)~~Annoni et al. (2015); Gebraad et al. (2016)). Wake steering typically uses yaw misalignment of the turbines to redirect the wake around downstream turbines. Various computational fluid dynamics ~~(CFD)~~ simulations and wind tunnel experiments have shown that this method can increase power without substantially increasing turbine loads (Gebraad et al. (2016); Fleming et al. (2014); Jiménez et al. (2010)). Yaw-based wake steering control has also been used in optimization studies of turbine layouts to improve the annual energy production of a wind ~~farm~~ plant (Fleming et al. (2016); Thomas et al. (2015); Stanley et al. (2017)). Recent CFD studies have determined that the shape of the wake and atmospheric stability are significant factors in wake steering (Vollmer et al. (2016)).

Control-oriented models are essential for developing and deploying wake steering strategies in wind farms. In particular, control-oriented models can be used in open-loop ~~control~~ where a look-up table is generated a priori and used in the field. Alternatively, ~~because of~~ due to its computational efficiency, a control-oriented model can be used to perform online optimization with feedback to adjust to changing conditions in the atmosphere or wind farm, ~~(~~e.g. turbine down for maintenance~~)~~. Lastly, control-oriented models are also useful for large-scale analysis and assessing the impact of controls~~and~~/optimization on annual energy production. Overall, these models are critical to the success of wind farm controllers and as a result, full-scale validation of these control-oriented models is essential and a high priority in this area of research.

A full-scale demonstration of wake steering is necessary to understand ~~its advantages~~ the benefits of wake steering and to validate the benefits predicted by simulations. Wind tunnel tests have been conducted that show encouraging results that match simulation results based on wake redirection (Campagnolo et al. (2016); Schottler et al. (2016)). In addition, there are preliminary results of the benefits of wake steering from an offshore commercial wind ~~farm~~ plant (Fleming et al. (2017c)). ~~NREL~~ The National Wind Technology Center also conducted a detailed full-scale demonstration in which a utility-scale turbine ~~was~~ operated at various yaw offsets while the wake was measured using a scanning lidar. In this paper, the lidar data collected from this campaign ~~are~~ is used to validate controls-oriented tools that are used for wind ~~farm~~ plant control. The main contributions of this work include a review of control-oriented models used for wake steering as well as a ~~quantitatively comparing these models and~~ quantitative analysis of these models with respect to full-scale lidar results. The results between the wake models and lidar data show good agreement under various atmospheric and turbine operating conditions, ~~as~~ shown in Section 4. This is an encouraging result that provides confidence in previously reported benefits of wake steering. The wind ~~farm~~ plant control tools, including wake models, turbine models, and lidar models, used in wind ~~farm~~ plant controls are introduced in Section 2. The field campaign is briefly introduced in Section 3. Finally, Section 5 provides conclusions and future work.

2 Modeling

~~FLOw Redirection and Induction in Steady State (FLORIS)~~ FLORIS is defined as a set of controls and optimization tools used for wind farm control developed at ~~NREL~~ the National Renewable Energy Laboratory and TU Delft~~(~~, see Figure 1~~)~~. This tool

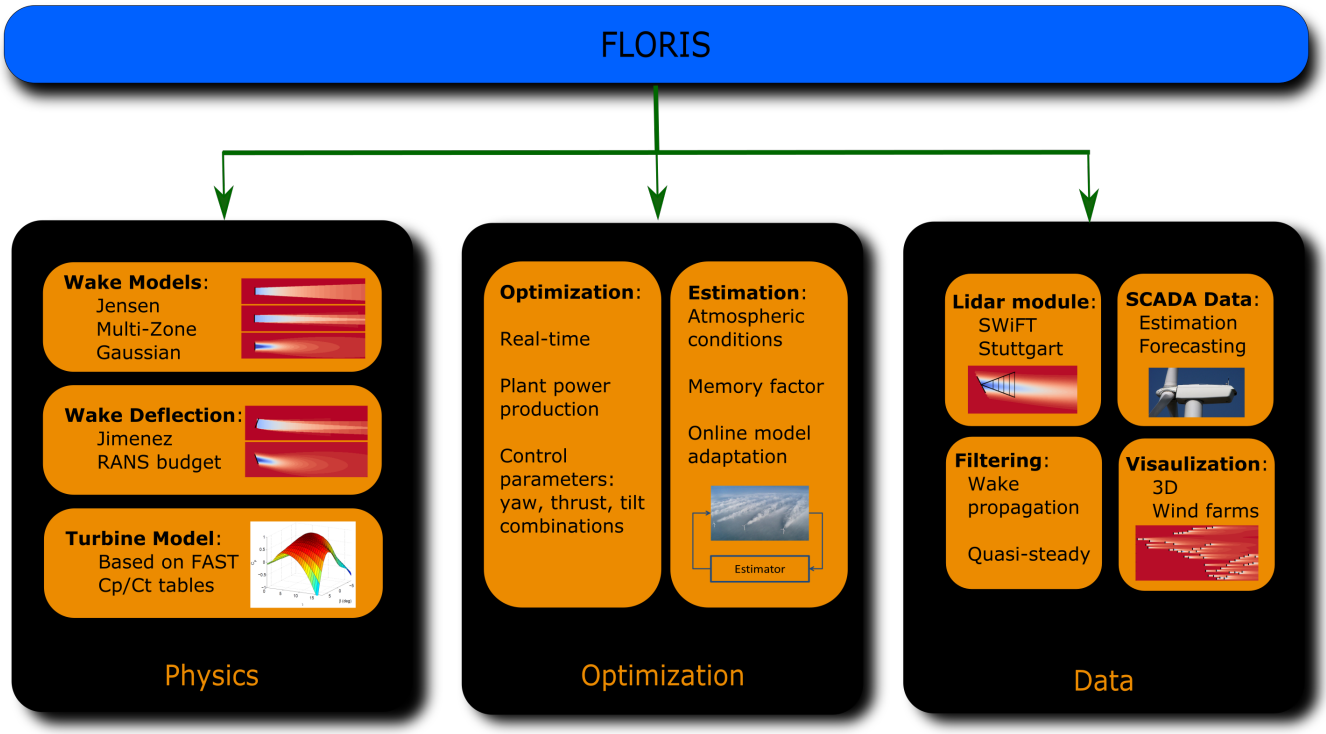

Figure 1. ~~The~~ FLORIS toolset is comprised of three main sections: (1) ~~physics~~Physics, (2) ~~optimization~~Optimization, and (3) ~~data~~Data.

models the turbine interactions in a wind ~~farm~~ plant and can be used to perform real-time optimizations to improve wind ~~farm~~ plant performance and integrate ~~supervisory and data acquisition data (SCADA)~~ SCADA data collected at wind ~~farms~~plants. This section focuses on the wake models, turbine models, and the lidar ~~model~~ module used in this paper.

2.1 Wake Model

The wake models available in FLORIS include the Jensen ~~model~~ Model (Jensen (1983)), the ~~multizone~~ FLORIS wake model (Gebraad et al. (2016)), and the self-similar wake model with contributions from ~~(Bastankhah and Porté-Agel (2014, 2016); Abkar and Port~~ Although only these three ~~wake~~ models are addressed~~and implemented in FLORIS~~, any wake model can be substituted into ~~the FLORIS frameworkfor real-time optimization of a wind farm~~this framework. This paper also demonstrates the modular framework for FLORIS and will address the benefits of adding complexity to wake models used to characterize the aerodynamic interactions between turbines.

2.1.1 Jensen Model

The Jensen model has been used for numerous studies on wind ~~farm~~ plant controls (Jensen (1983); Johnson et al. (2006); Katic et al. (1986)). This model has a low computational cost ~~because of~~ due to its simplicity and is based on assumptions that there

is a steady inflow~~and ,~~ linear wake expansion, and ~~that~~ the velocity in the wake is uniform at a cross section downstream. The turbine is modeled as an actuator disk with uniform axial loading in a steady uniform flow.

Consider the example of a turbine operating in ~~free stream~~ freestream velocity, U_∞. The diameter of the turbine rotor plane is denoted by D and the turbine is assumed to be operating at an induction factor, a. A cylindrical coordinate system is placed at the rotor hub of the first turbine with the streamwise and radial distances denoted by x and r, respectively. The velocity profile at a location (x, r) is computed as:

$$u(x, r, a) = U_\infty(1 - \delta u(x, r, a)) \tag{1}$$

where the velocity deficit, δu, is given by:

$$\delta u = \begin{cases} 2a\left(\frac{D}{D+2kx}\right)^2, & \text{if } r \leq \frac{D+2kx}{2}. \\ 0, & \text{otherwise.} \end{cases} \tag{2}$$

In this model, the velocity, u, is defined in the axial (x) direction and the remaining velocity components are neglected. The wake is parameterized by a tuneable ~~nondimensional~~ nondimnensional wake decay constant, k. Typical values of k range from 0.01 to 0.5 depending on ambient turbulence, topographical effects, and turbine operation. For example, if the ambient turbulence is high, then the wakes within the wind farm will ~~recover faster because of the mixing with the atmospheric flow~~recovery faster due to the mixing of the wake. As a result, the k value will be higher indicating that the wake will recover faster. There is no standard ~~numerical~~ rule for how k varies with turbulence intensity.

Limitations: The ~~Jensen~~ Park model can be used to compute the power production and velocity deficit of a turbine array. This ~~model has been used to determine~~ is useful in determining operating conditions of a wind farm to maximize power~~(Johnson and Thomas (2009))~~. However, ~~the model neglects the effects~~ it has no notion of added turbulence in the downstream wake ~~as a result of~~ due to varying turbine operation. The ~~model~~ assumptions are based on a steady inflow acting on an actuator disk with uniform axial loading and as noted in **?**, the Jensen model does not conserve momentum. Despite its limitations, the Jensen model can be computed in fractions of a second and can provide some insight ~~into turbine interaction in a short amount of time.~~ of turbine interaction that can be used to understand the results obtained from higher-fidelity models In addition, if uncertainty is included, the Jensen model performs well and ~~successfully~~ predicts wake interactions well under normal operating conditions.

2.1.2 ~~Multizone Model~~Multi-Zone

The ~~multizone~~ multi-zone model, developed in (Gebraad and Van Wingerden (2014)), is a modification of the Jensen model described in the previous section. Modifications were made to ~~Jensen~~ better model the wake velocity profile and effects of partial wake overlap, especially in yawed conditions. The ~~multizone~~ multi-zone model defines three wake zones, q: (1) ~~near-wake~~

near wake zone, (2) ~~far-wake~~ far wake zone, and (3) ~~mixing-wake~~ mixing wake zone. The effective velocity at the downstream turbine ~~,~~i ~~,~~is found by combining the effects of each of the wake zones of the upstream turbine ~~,~~j:

$$u_i = U_\infty \left(1 - 2\sqrt{\sum_j \left[a_j \sigma^3_{q=1} c_{j,q} (X_i \min(\frac{A^{\text{overlap}}_{j,i,q}}{A_i}, 1)) \right]^2} \sqrt{\sum_j \left[a_j \sigma^3_{q=1} c_{j,q} (X_i \min(\frac{A^{overlap}_{j,i,q}}{A_i}, 1)) \right]^2} \right) \tag{3}$$

where X_i is the x location of turbine i, ~~$A^{\text{overlap}}_{j,i,q}$~~ $A^{overlap}_{j,i,q}$ is the overlap area of a wake zone, q of a turbine i with the rotor of turbine j, and $c_{i,q}(x)$ is a coefficient that defines the recovery of a zone q to the ~~free stream~~ freestream conditions:

$$c_{i,q}(x) = \left(\frac{D_i}{D_i + 2k_e m_{U,q}(\gamma_i)[x - X_i]} \right)^2 \tag{4}$$

where $m_{U,q}$ is defined as:

$$m_{U,q}(\gamma_i) = \frac{M_{U,q}}{\cos(a_U + b_U \gamma_i)} \tag{5}$$

~~where~~ for $q = 1, 2, 3$ corresponding to the three wake overlap zones, where a_U and b_U are tuned model parameters, D_i is the rotor diameter of turbine i, γ_i is the yaw offset of turbine i, and $M_{U,q}$ are tuned scaling factors that ensure that the velocity in the outer zones of the wake will recover to the ~~free stream~~ freestream conditions faster than the inner zone. The parameters of the model were tuned to match the results from high-fidelity wake simulations (Gebraad et al. (2016)) . The most influential parameter is k_e, because it defines both wake expansion and wake recovery. Additional details can be found in (Gebraad et al. (2016)).

Limitations: The ~~multizone model was tuned~~ multi-zone model was developed, in comparison with high-fidelity models, to characterize turbine interactions when turbines were operating in partial wake or yawed conditions. The ~~multizone~~ multi-zone model is a computationally inexpensive model that in suitable for ~~online~~ controls and optimization studies to improve wind ~~farm~~ plant performance. However, there are ~~ten~~ 13 free parameters that can be tuned in this model and the tuning can be sensitive depending on the parameters chosen to tune. Like the Jensen model, this model does not have any sensitivity to turbulence intensity or added turbulence generated by an upstream turbine and does not explicitly conserve momentum.

2.1.3 Gaussian Model

Lastly, a Gaussian model is incorporated in the overall FLORIS wake modeling and controls tools. This model was introduced by several recent papers including (~~Abkar and Porté-Agel (2015); Bastankhah and Porté-Agel (2014, 2016); Niayifar and Porté-Agel (2016~~ This model includes a Gaussian wake ~~, in the y and z directions,~~ to describe the velocity deficit, added turbulence based on turbine operation, and atmospheric stability.

Velocity Deficit: The velocity deficit of a wake is computed ~~using~~ by assuming a Gaussian wake, which is based on self-similarity theory often used in free shear flows, (Pope (2000)). An analytical expression for the three-dimensional velocity deficit behind a turbine in the far wake can be derived from the simplified Navier-Stokes equations as:

$$\frac{u(x,y,z)}{U_\infty} = 1 - Ce^{-(y-\delta)^2/2\sigma_y^2} e^{-(z-z_h)^2/2\sigma_z^2} \tag{6}$$

$$C = 1 - \sqrt{1 - \frac{(\sigma_{y0}\sigma_{z0})M_0}{\sigma_y \sigma_z}}$$

$$M_0 = C_0(2 - C_0)$$

$$C_0 = 1 - \sqrt{1 - C_T}$$

where C is the velocity deficit at the wake center, δ is the wake deflection (see Section 2.2), z_h is the hub height of the turbine, σ_y defines the wake width in the y direction, ~~and~~ σ_z defines the wake width in the z direction. Each of these parameters are defined with respect to turbine i; subscripts are excluded for brevity. The subscript "0" refers to the initial values at the start of the far wake, which is dependent on ambient turbulence intensity, I_0, and the thrust coefficient, C_T. For additional details on ~~near-wake calculations, refer~~ near wake calculations, the reader is referred to (Bastankhah and Porté-Agel (2016)). Abkar and Porté-Agel (2015) ~~demonstrate~~ demonstrates that σ_y and σ_z grow at different rates based on lateral wake meandering (y-direction) and vertical wake meandering (z-direction). The velocity distributions σ_z and σ_y are defined as:

$$\frac{\sigma_z}{d} = k_z \frac{(x - x_0)}{d} + \frac{\sigma_{z0}}{d}, \qquad \text{where } \frac{\sigma_{z0}}{d} = \frac{1}{2}\sqrt{\frac{u_R}{u_\infty + u_0}} \tag{7}$$

$$\frac{\sigma_y}{d} = k_y \frac{(x - x_0)}{d} + \frac{\sigma_{y0}}{d}, \qquad \text{where } \frac{\sigma_{y0}}{d} = \frac{\sigma_{z0}}{d}\cos\gamma \tag{8}$$

where k_y defines the wake expansion in the lateral direction and k_z defines the wake expansion in the vertical direction. For this study, k_y and k_z are set to be equal and the wake expands at the same rate in the lateral and vertical directions. The wakes are combined using the traditional sum of squares method (Katic et al. (1986)), although alternate methods are proposed in ~~Niayifar and Porté-Agel (2016)~~Niayifar and Porté-Agel (2015).

Atmospheric ~~Conditions~~Stability: This model also accounts for physical atmospheric quantities such as shear, veer, and changes in turbulence intensity (~~Abkar and Porté-Agel (2015); Niayifar and Porté-Agel (2016)~~Abkar and Porté-Agel (2015); Niayifar and Shear, veer, and turbulence intensity measurements are typically available in field measurements and will be used to characterize atmospheric ~~conditions~~ stability in this particular model. ~~These are physical parameters that can be available in field measurements.~~ It should be noted that these three parameters do not sufficiently characterize atmospheric stability as defined in Stull (2012). Other parameters ~~,~~ such as vertical flux and temperature profiles ~~,~~ are necessary to fully capture atmospheric stability.

~~The Gaussian~~ This model is a three-dimensional wake model that includes shear by using the power log law of wind:

$$\frac{u}{U_\infty}\frac{U_{init}}{U_\infty} = \left(\frac{z}{z_{hub}}\right)^{\alpha_s} \tag{9}$$

where α_s is the shear coefficient and U_{init} indicates the initial flow field. A high shear coefficient, $\alpha_s > 0.2$, ~~is typically~~ typically is used for stable conditions and a low shear coefficient, $\alpha_s < 0.2$, is typically used for unstable conditions (Stull (2012)).

This wake model also takes into account veer associated with wind direction change across the rotor. A rotation factor is added to the Gaussian wake (6) such that:

$$\frac{u(x,y,z)}{U_\infty}\frac{u(x,y,z)}{U_{init}} = 1 - Ce^{-(a(y-\delta)^2 - 2b(y-\delta)(z-z_{hub}) + c(z-z_{hub})^2)} \tag{10}$$

$$a = \frac{\cos^2\phi}{2\sigma_y^2} + \frac{\sin^2\phi}{2\sigma_z^2}$$

$$b = -\frac{\sin 2\phi}{4\sigma_y^2} + \frac{\sin 2\phi}{4\sigma_z^2}$$

$$c = \frac{\sin^2\phi}{2\sigma_y^2} + \frac{\cos^2\phi}{2\sigma_z^2}$$

where ϕ is the amount of veer ~~, i.e. change in wind direction,~~ across the rotor ~~. This~~ where this equation represents a standard Gaussian rotation.

Lastly, turbulence intensity is accounted for in the model by linking ambient turbulence intensity to wake expansion. An empirical relationship is provided in ~~Niayifar and Porté-Agel (2016)~~Niayifar and Porté-Agel (2015):

$$k_y = 0.38371I + 0.003678 \tag{11}$$

where I represents the ~~streamwise turbulence intensity~~turbulence intensity, k_a and k_b are tuning parameters where $k_a = 0.38371$, and $k_b = 0.003678$ in Niayifar and Porté-Agel (2015). As stated previously, k_y and k_z ~~are considered~~ will be set equal in this study.

Added Turbulence: This wake model also computes added turbulence generated by turbine operation and ambient turbulence conditions. For example, if a turbine is operating at a higher thrust, this will cause the wake to recover faster. Conversely, if a turbine is operating at a lower thrust, this will cause the wake to recover slower. Conventional linear flow models have a single wake expansion parameter that does not change under various turbine operating conditions. ~~Niayifar and Porté-Agel (2016)~~ Niayifar and Po a model that incorporated added turbulence ~~caused by~~ due to turbine operation:

$$I = \sqrt{\sum_{j=0}^{N}(I_j^+)^2 + I_0^2} \tag{12}$$

where N is the number of turbines influencing the downstream turbines, I_0 is the ambient turbulence intensity, and the added turbulence ~~caused by~~ due to turbine i, I_i^+ is computed as:

$$I^+ = A_{overlap}\left(0.8a_i^{0.73}I_0^{0.35}(x/D_i)^{-0.32}\right) \tag{13}$$

where I_0 is the ambient turbuence intensity and a is the axial induction factor of the turbine, which can be defined in terms of C_T based on Burton et al. (2001); Bastankhah and Porté-Agel (2016):

$$a \approx \frac{1}{2\cos\gamma}\left(1 - \sqrt{1 - C_T\cos\gamma}\right)$$

In ~~Niayifar and Porté-Agel (2016)~~Niayifar and Porté-Agel (2015), the number of turbines, N, used to determine the added turbulence is $N = 1$~~where the one turbine is the turbine with the strongest wake effect on the turbine being evaluated. In the formulationused in FLORIS~~. In this formulation, N is determined ~~by the number of turbines~~ based on a pre-defined distance to the downstream turbine rather than only including the influence of one turbine. For example, ~~the model included in FLORIS arbitrarily~~ this model considers contributions to the added turbulence intensity from turbines within 15D. This has shown to be beneficial ~~,~~ especially with closely spaced turbines. Studies have shown that the added turbulence intensity has reached an equilibrium point between two and three turbines downstream (Chamorro and Porté-Agel (2011)).

~~**Capabilities and** **Limitations:**~~ ~~The Gaussian~~ This wake model is an analytical model with approximations made from the ~~simplified~~ steady-state Navier-Stokes equations based on free shear flows. In addition, unlike the previous two models, this model conserves momentum. However, it relies on a linear wake expansion model and has six tuning parameters based on empirical relationships for wake expansion and turbulence intensity (Equations 11 and 13). The main benefits of this model come from the ties to physical measurements in the field such as shear, veer, and turbulence intensity and its roots in ~~self-similar~~ free shear flow theory.

2.2 Wake Deflection

The wake models defined ~~earlier~~ above include wake deflection models that approximate the amount of lateral movement based on yaw misalignment of the turbine. ~~It is important to note that when a turbine is positively misaligned, the turbine has rotated counter-clockwise to be misaligned with the oncoming wind (conventional right-hand-rule).~~ Two wake deflection models are defined in the FLORIS wind ~~farm~~ plant modeling and controls framework and are briefly described in this section.

2.2.1 Jimenez Model

An empirical formulation was presented in Jiménez et al. (2010) and used in the ~~multizone~~ multi-zone formulation (Gebraad et al. (2016)). When a turbine is yawed, it exerts a force on the flow that causes the wake to deflect and deform in a particular direction. The angle at the wake centerline is defined as:

$$\xi(x) \approx \frac{\xi_{init}^2}{1 + 2k_d \frac{x}{D}} \tag{14}$$

$$\xi_{init}(a, \gamma) = \frac{1}{2} \cos^2 \gamma \sin \gamma C_T$$

where ξ_{init} is the initial skew angle from the wake centerline and k_d is a tuneable deflection parameter. In Gebraad et al. (2016), the wake deflection angle is integrated to determine the amount of deflection, ~~and~~ δ achieved by yaw misalignment in the spanwise (y direction):

$$\delta(x) = \int_0^x \tan \xi(x) dx \tag{15}$$

$$\delta(x) \approx \frac{\xi_{init} \left(15 \left(\frac{2k_d x}{D} + 1 \right)^4 + \xi_{init}^2 \right)}{\frac{30k_d}{D} \left(\frac{2k_d x}{D} + 1 \right)^5} - \frac{\xi_{init} D \left(15 + \xi_{init}^2 \right)}{30k_d}$$

The deflection, δ, is achieved by integrating a second-order Taylor series approximation shown in Gebraad et al. (2016).

2.2.2 Bastankhah ~~and Porte-Agel~~ Model

In Bastankhah and Porté-Agel (2016), the wake deflection due to yaw misalignment of turbines is defined by doing budget analysis on the Reynolds Averaged Navier-Stokes equations. The wake deflection angle at the rotor is defined by:

$$\theta \approx \frac{0.3\gamma}{\cos\gamma}\left(1-\sqrt{1-C_T\cos\gamma}\right) \tag{16}$$

and the initial wake deflection, δ_0 is defined as:

$$\delta_0 = x_0 \tan\theta \tag{17}$$

where x_0 is the length of the ~~near-wake~~ near wake as defined in Bastankhah and Porté-Agel (2016). The total deflection of the wake ~~as a result of~~ due to wake steering is defined as:

$$\delta = \delta_0 + \frac{\theta E_0}{5.2}\sqrt{\frac{\sigma_{y0}\sigma_{z0}}{k_y k_z M_0}}\ln\left[\frac{(1.6+\sqrt{M_0})\left(1.6\sqrt{\frac{\sigma_y\sigma_z}{\sigma_{y0}\sigma_{z0}}}-\sqrt{M_0}\right)}{(1.6-\sqrt{M_0})\left(1.6\sqrt{\frac{\sigma_y\sigma_z}{\sigma_{y0}\sigma_{z0}}}+\sqrt{M_0}\right)}\right] \tag{18}$$

where $E_0 = C_0^2 - 3e^{1/12}C_0 + 3e^{1/3}$. Expressions for the other symbols in ~~(??)~~ the above equation are provided in Section 2.1.3. See Bastankhah and Porté-Agel (2016) for details on the derivation.

2.2.3 Wake Asymmetry

Wake deflection is known to be asymmetric based on the sign of the yaw misalignment. In particular, positive yaw angles are more effective than negative yaw angles Fleming et al. (2017a). Previously, it was speculated that there was a rotation-induced lateral offset that is caused by the interaction of the wake rotation with the shear layer (Gebraad et al. (2016)). An empirical correction used to account for asymmetry is presented in Gebraad et al. (2016).

Fleming et al. (2017a) proposes that there is an asymmetry in the wake that can be described by counter-rotating vortices, turbine rotation, and shear rather than actual deflection. Updates to the FLORIS wake modeling framework to reflect the asymmetry will be done in future work.

2.3 Turbine Model

In addition to wake modeling tools, a turbine model is used in the wind ~~farm~~ plant tools to provide a realistic description of turbine interactions in a wind ~~farm~~plant. The turbine model consists of a C_P/C_T table based on wind speed and constant blade pitch angle generated by ~~a blade-element momentum code,~~ FAST (Jonkman (2010)). The coupling between C_P and C_T is critical in understanding the benefits of wind ~~farm~~ plant controls. C_P and C_T ~~can~~ also be coupled using actuator disk theory, which is based on the turbine operation defined by an axial induction factor, a:

$$C_P = 4a(1-a)^2 \tag{19}$$

$$C_T = 4a(1-a)$$

It is important to note that C_P and C_T values are used that correspond to the local conditions each turbine is operating in. For example, a turbine operating in a wake has a different C_P/C_T than a turbine operating in ~~free stream~~ freestream conditions.

The steady-state power of each turbine under yaw misalignment conditions is given by (Gebraad et al. (2016)):

$$P = \frac{1}{2}\rho A C_P \cos\gamma^p u^3 \tag{20}$$

where p is a tuneable parameter that matches the power loss due to yaw misalignment seen in simulations. In actuator disk theory (Burton et al. (2001)), $p = 3$. However, based on large-eddy simulations, the turbine power in yaw misalignment has been shown to match the output when $p = 1.88$ for the NREL 5 MW~~Jonkman et al. (2009)~~. Field observations ~~were~~ run from $p = 1.4$ (Fleming et al. (2017c)) to $p = 2.2$.

2.4 Lidar Model

Finally, in this work a lidar model has been added to the FLORIS wind ~~farm framework~~plant tools. This lidar model is based on the scanning lidar used at the University of Stuttgart ~~'s scanning lidar~~ used in this study. This ~~approach~~ allows for direct comparison between lidar data collected by the scanning lidar and the wake model used. In particular, the scanning lidar used in the field campaign takes a weighted average of nine points along the line-of-sight trajectory. A lidar model is necessary to ensure this direct comparison. If any of the nine points are outside of the wake, the weighted average may lead to a more conservative estimate of the flow in the wake. More details on the lidar used in the wake steering campaign can be found in Raach et al. (2016); Fleming et al. (2017b); Raach et al. (2017).

The velocity computed by the scanning lidar is based on a line-of-sight velocity. The lidar model used in the FLORIS framework computes the line-of-sight velocity, v_{LOS}, in the same way that the lidar model computes the ~~line-of-sight~~ line of sight velocity so that each point that is scanned by the lidar can be compared directly to points computed by the wake model. The lidar computes a line-of-sight velocity for each point scanned. In particular, one scan point consists of $N_{weights}$ weighted points that provide a robust velocity measurement at that location. In other words, $N_{weights}$ points are used in a weighted sum to provide a robust velocity measurement at that scan point. The velocity at a single point can be computed as:

$$\boldsymbol{u}_i = \sum_{j=0}^{N_{weights}} a_j \tilde{\boldsymbol{u}}_{\boldsymbol{p}j} \tag{21}$$

where a_j represents the weights ~~, which are~~ assigned to each point, i indicates the scan point, and $\boldsymbol{u} = [u_i, v_i, w_i]^T$ is the weighted sum of the measured velocity points ~~,~~$\tilde{\boldsymbol{u}}_p$. Typically ~~,~~the weights are assigned in a Gaussian manner.

Furthermore, the wind vector ~~,~~$\boldsymbol{u} = [u_i, v_i, w_i]^T$ ~~,~~is projected onto the normalized laser vector point $[x_i, y_i, z_i]^T$ with a focus distance of $f_i = \sqrt{x_{i,I}^2 + y_{i,I}^2 + z_{i,I}^2}$ and the resulting $v_{LOS,i}$ ~~being~~is:

$$v_{los,i} = \frac{x_{i,I}}{f_i} u_{i,I} + \frac{y_{i,I}}{f_i} v_{i,I} + \frac{z_{i,I}}{f_i} w_{i,I} \tag{22}$$

Additional details are provided in Raach et al. (2016). This model can be used in conjunction with the field data to perform closed-loop wind ~~farm controls , as performed~~ plant controls as is done in Raach et al. (2016). In addition, ~~future~~ Future work could use the simulated v_{LOS} ~~, which is~~ computed using this lidar model to fill in gaps that are inevitably present in real-time lidar data.

3 Field Campaign

A wake steering demonstration was conducted at ~~NREL's~~ the National Wind Technology Center ~~(NWTC)~~ using a utility-scale turbine. The utility-scale turbine operated at various yaw misalignment conditions and the resulting wake was ~~continuously~~ continually recorded by a nacelle-mounted lidar. The campaign started in September 2016 and concluded in April 2017. This section describes the turbine, the meteorological tower used to record local conditions, and the lidar system mounted on the nacelle of the turbine. Details were first reported on the lidar field campaign in Fleming et al. (2017b). This paper expands the analysis and ~~quantitatively compares~~ provides a quantitative comparison between the control-oriented models presented and the lidar data collected in this campaign.

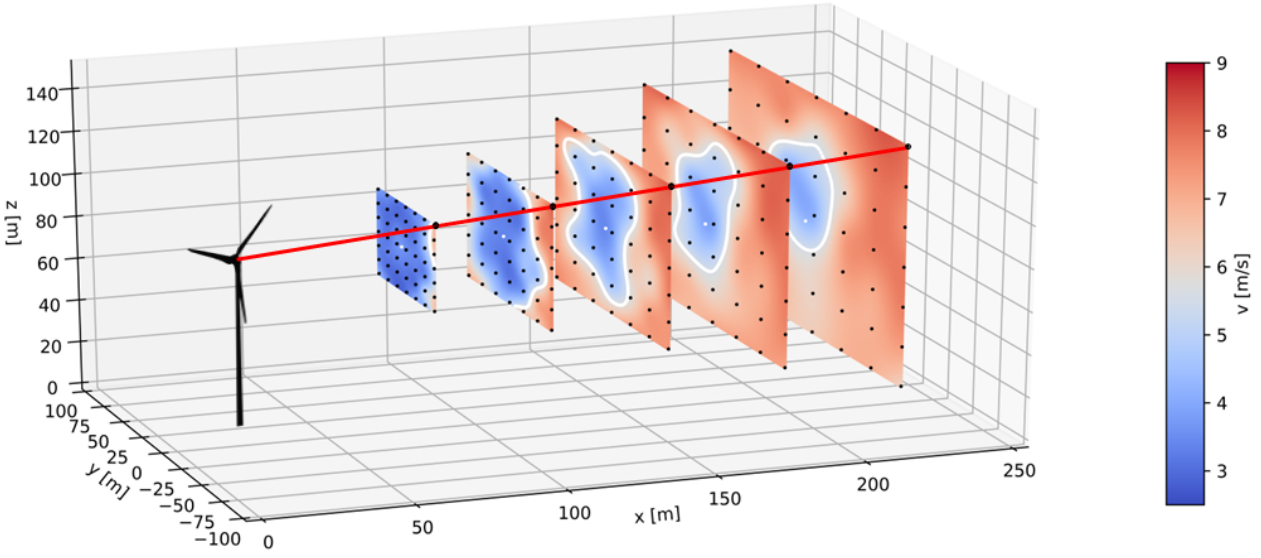

Figure 2. Lidar scan pattern used at the ~~five~~ 5 locations downstream of the turbine.

3.1 Setup of the Field Campaign

The turbine used in this wake steering demonstration was the ~~U.S.~~ Department of Energy (DOE) 1.5 MW GE SLE turbine ~~operated by NREL (Mendoza et al. (2015); Santos and van Dam (2015); Roadman and Huskey (2015))~~owned by the U.S. DOE and operated by the National Renewable Energy Laboratory. Details of the turbine are provided in Table 1.

Table 1. Test Turbine Details.

Rated Power (kW)	1500
Hub Height (m)	80
Nominal Rotor Diameter (m)	77
Rated Wind Speed (m/s)	14

The ~~meteorological (met)~~ met tower is located 161 m upstream of the turbine in the predominant wind direction~~and~~ . The met tower was instrumented in accordance with ~~International Electrotechnical Commission~~ IEC 61400-12-1. Table 2 lists the instrumentation used on the met tower. The turbine nacelle wind speed and wind direction are measured and recorded and synchronized with the met tower data.

Table 2. Meteorological Tower Instrumentation Details.

Instrument	Elevations (m)
Precipitation	1
Wind Speed	38, 55, 80, 87, 90, 92
Wind Direction	38, 87
Humidity	90
Temperature	38, 90
Barometric Pressure	90

The lidar data ~~analyzed in this paper are~~ is limited to a region in which the met tower is upstream of the turbine. The hub-height wind speed and wind direction measurements from the met tower are used to described the mean wind speed, wind direction, and turbulence intensity. The wind direction ~~measurements~~ recorded at 38 m and 87 m on the met tower are used to compute veer.

3.2 Lidar Specifications

The University of Stuttgart scanning lidar system consists of two parts: (1) a ~~pulsed~~ Windcube V1 from Leosphere and (2) a scanner unit developed at the University of Stuttgart. A two-degree of freedom mirror is used for redirecting the beam to

any position within the physical limitations of the mirror. The lidar can scan an area of ~~(~~0.75~~D~~ D × 0.75~~D), up to 2.8D downstream~~ D using up to 49 measurement points and five scan distances. The scan rate is dependent on the number of pulses used for each measurement position. The lidar system has been used for lidar-assisted control ~~by applying~~ using inflow and wake measurements~~(see Raach et al. (2016))~~, see Raach et al. (2016).

The lidar scans a grid pattern ~~shown~~ seen in Figure 2~~and~~ . The lidar is set to record a measurement point every 1 s ~~on~~ and it scans five distances from ~~1D~~ 1D to 2.8~~D~~ D simultaneously. Each scan consists of 49 points and one scan takes 48 s on average. At each measurement point the lidar uses 10,000 laser pulses to measure the line-of-sight wind speed, v_{LOS}, described in Section 2.4. Scans of similar atmospheric conditions and turbine operation are aggregated to produce a mean or median scan.

4 Results

The results presented in this section show the comparison between the wake models described in Section 2 and the lidar data collected in the field campaign described ~~in~~ Section 3. The results focus on comparisons of the velocity deficit behind the turbine, the wake deflection achieved in yaw misalignment conditions, and ~~the impact of~~ varying atmospheric conditions.

4.1 Data Processing

It is important to note how the lidar data ~~were~~ was processed for this study. The lidar data ~~were~~ was first processed to filter out implausible data. Specifically, several methods were applied to check for hard target measurements, filter out lidar data with a bad carrier-to-noise ratio, and check for plausibility of the measurement data. The data is also reduced ~~to only include~~through certain considerations including: (1) periods where the met tower is upstream of the turbine~~to avoid blockage effects~~, (2) periods where the turbine is producing at least 100 kW~~to capture known wake effects~~, and (3) periods where difference between the target and realized yaw misalignment is small. In particular, the instruments on the met tower that are used to measure wind speed and direction are more reliable when they are not operating in the wake of nearby turbines or in the wake of its own tower due to blockage effects. We also chose to only include data where the turbine is operating normally. In this case, we define that as producing more than 100 kW. The turbine operation affects the wake properties and we need to ensure that we are comparing times when the turbine is performing as expected. Similarly, we only include times when the turbine yaw controller is tracking the specified offset within a few degrees to make a direct comparison with models.

4.2 Atmospheric Conditions

First, the lidar data collected in the field campaign ~~were~~ was analyzed based on atmospheric conditions. In particular, turbulence intensity was examined to understand the behavior of each model under varying turbulence intensity conditions. Figure 3 shows the lidar scans at ~~2.35D~~180.95 m downstream (approximately 2.5D downstream). The turbulence intensity was computed for each lidar scan and separated into four bins with centers of 2%, 6%, 10%, and 14% with a wind speed of 8 m/s. Figure 3 shows that the wake is strongest in ~~low-turbulence~~ low turbulence conditions and dissipates quickly in ~~high-turbulence~~ high turbulence conditions. This ~~result~~ is consistent with previous work investigating the effects of atmospheric conditions on wakes

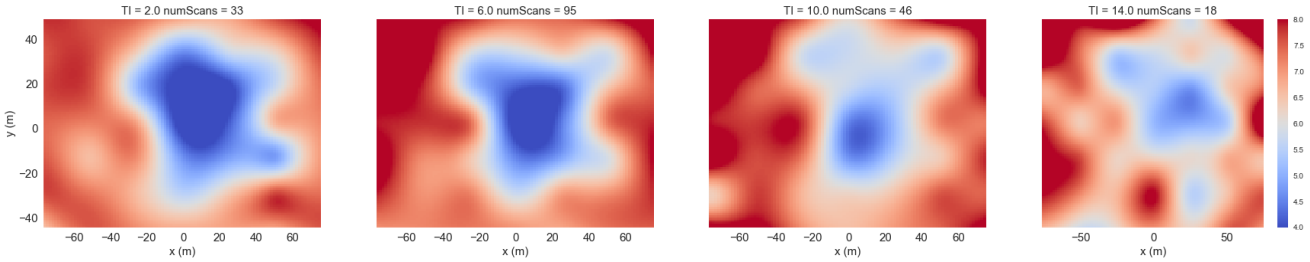

Figure 3. Lidar data at ~~2.35*D*~~ 180.95 m downstream at different turbulence intensities ranging from 2.0 % to 14.0 %~~at 8 m/s~~. The title of each plot indicates the turbulence intensity and the number of scans ~~(*numScans*)~~ used to produce each time-averaged figure.

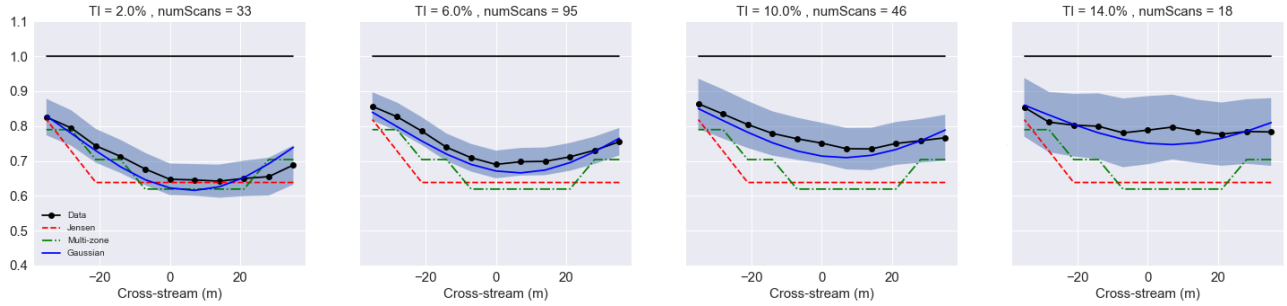

Figure 4. Velocity deficit at ~~2.35*D*~~ 180.95 m downstream computed using lidar data, the Gaussian wake model, ~~multizone~~ multi-zone wake model, and the Jensen wake model under different turbulence intensity conditions.

(Smalikho et al. (2013)). It is important to note that each image was generated with the maximum number of scans available after processing the data. More scans lead to a more robust measurement of the wake. A statistical analysis is presented in Figure 4, which indicates the effects of the limited number of scans processed.

Figure 4 shows how the controls-oriented engineering models presented in this paper compare with the lidar data. ~~Each model was tuned to a subset of the lidar data which included primarily low-turbulence intensity data with a mean turbulence intensity of approximately 5%.~~ The velocity deficit behind the turbine was computed by averaging the velocity across a "virtual" rotor and moving this rotor across the domain in the spanwise direction (shown in Vollmer et al. (2016)). The bands indicate a 95 % confidence interval. A larger band indicates that fewer scans were processed. Each model was tuned to a subset of the lidar data which included primarily low turbulence intensity data with a mean turbulence intensity of approximately 5%. The values of each of the model parameters are shown in the Appendix. It is important to note that these values are tuned for the near wake due to the close proximity of the lidar scans to the turbine (2.35D). Although these measurements are near the turbine, the effects of turbulence intensity can still be observed along with wake deflection. Tuning the models appropriately with training data from this proximity, the models are able to perform reasonably well under varying atmospheric conditions and varying turbine operations even at these close proximities.

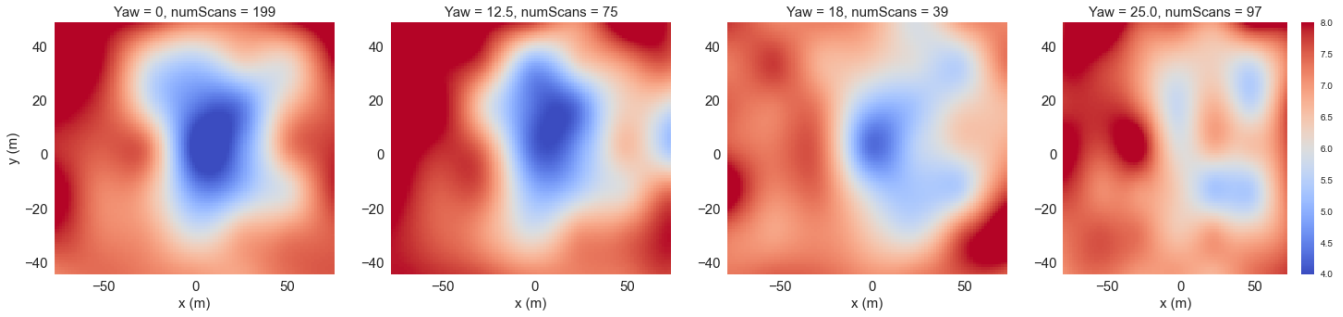

Figure 5. Lidar data at ~~2.35*D*~~ 180.95 m downstream at different yaw misalignments ranging from 0° to 25° ~~at 8 m/s~~. The title of each plot indicates the yaw angle and the number of scans used to produce each time-averaged figure.

Jensen and the ~~multizone~~ multi-zone wake models are shown to have good agreement in ~~low-turbulence scenarios(~~low turbulence scenarios, i.e. ~~,~~ they fall within the confidence interval~~). This outcome~~ . This is expected as these models were tuned to ~~low-turbulence~~ low turbulence scenarios. However, when ~~shifting~~ going to high turbulence intensity scenarios, ~~the models underpredict the~~ they under-predict the velocity deficit significantly. This is because neither the Jensen ~~nor the multizone~~ or the multi-zone model have turbulence intensity as an input to the model. The Gaussian model, however, is able to capture both ~~low- and high-turbulence intensity scenarios(~~low and high turbulence intensity scenarios, i.e. the model lies within the confidence interval bands under each turbulence scenario examined~~). This capability highlights the fact~~ . This highlights that, even under varying atmospheric conditions, the Gaussian model is able to accurately capture scenarios that it was not explicitly tuned for. The Jensen and multi-zone model can be retuned to fit high turbulence intensity data as well. Those values are also indicated in the Appendix.

4.3 Wake Deflection

Wake deflection was also analyzed using the lidar data from this campaign. Figure 5 shows the wake deflection under turbine yaw misalignment observed by the scanning lidar at ~~2.35*D*~~ 180.95 m downstream. Under larger yaw angles, the wake deflects and deforms as has been reported in (Howland et al. (2016); Fleming et al. (2017c)).

Figure 6 shows the comparison of each controls-oriented engineering model with the lidar data when the turbine is operating with no misalignment (left) and operating with 25° of yaw misalignment (right) at ~~2.35*D* downstream~~ 180.95 m downstream, or approximately 2.5D downstream. Similar to Figure 4, a "virtual" rotor is used to compute the effective wind speed at several spanwise locations. The data used in Figure 6 includes all ~~data collected in time periods when the wind speed was~~ turbulence intensity levels with wind speeds of 7-9 m/s ~~and~~ when the turbine was operating with no ~~yaw~~ misalignment and a yaw misalignment of 25°~~, regardless of turbulence intensity~~. The average turbulence intensity is approximately 7%. The data ~~were~~ was aggregated and normalized over this range of wind speeds to include more scans and provide more robust statistics. The bands indicate a 95 % confidence interval.

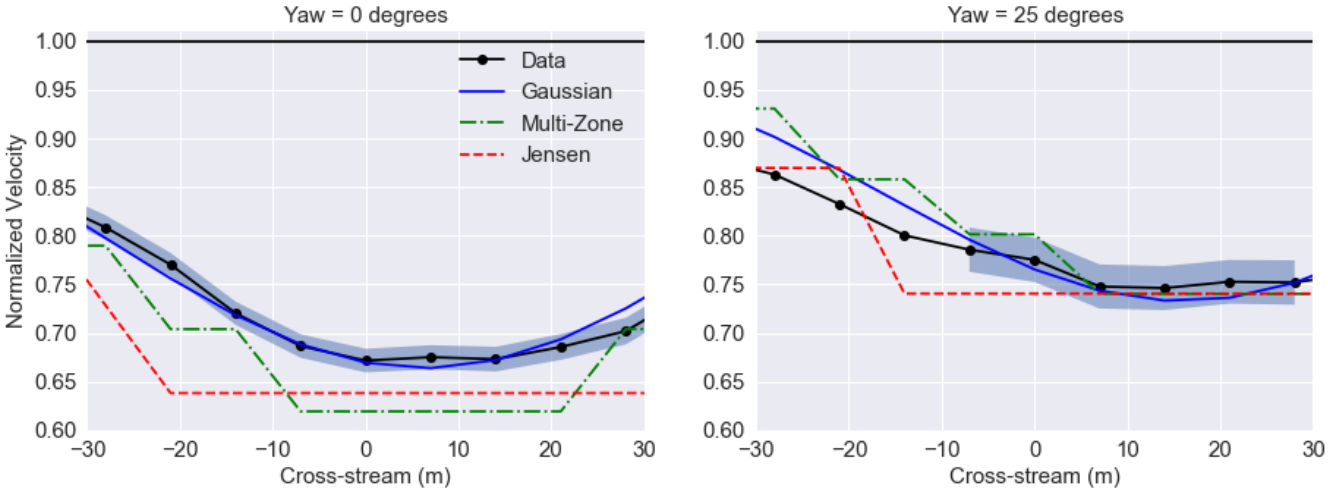

Figure 6. Velocity deficit at ~~2.35*D*~~ 180.95 m downstream computed using lidar data, the Gaussian wake model, the multi-zone wake model, and the Jensen wake model under different yaw misalignment conditions.

Again, the Gaussian model is better able to predict the conditions at no misalignment (predicts velocities within the confidence intervals) since the multi-zone and Jensen model were both tuned to data with a lower turbulence intensity. When the turbine is operating in misaligned conditions, the turbine generates a cross-flow velocity component that is not capture by the lidar. This is because the lidar is operating on a rotating platform and does not reliably measure the wake on the left side of the wake due to this large cross-flow velocity component. As a result, only lidar data from -10 m to 30 m is considered in the misaligned conditions. Under yaw misaligned conditions, the Jensen, multi-zone, and Gaussian model all have good agreement with lidar data under misaligned conditions. In this case, the Jensen and multi-zone wake models have better agreement under yawed conditions than under normal conditions. One potential reason for this is that the "depth" of the wake is modified by the changing yaw angle, i.e. the thrust generated by the turbine is modified. This modified thrust is able to accommodate the under predictions in the normal operating case. With more data, the analysis could be split into yaw misalignment conditions as well as turbulence intensity levels.

5 Conclusions and Future Work

~~This paper provides a quantitative analysis of wake models used~~

This paper compared field data from a scanning lidar measuring the wake of a turbine in normal operating conditions and yaw misaligned conditions with controls-oriented models. Validating these controls models with field data in a variety of conditions is a critical step to implementing wind farm controls in the field. A quantitative analysis was done comparing the models in the FLORIS framework ~~with respect to scanning lidar datacollected by NREL at the NWTC. Overall, the Gaussian wake model provides~~ to this data. The data was processed to look at the effects of varying turbulence intensity levels as well as different

yaw misaligned conditions. The wake models used in the comparison included the Jensen model, the multi-zone model, and the Gaussian wake mode. Future work will incorporate additional wake models that may be used in the context of wind farm controls. The Gaussian model provided the best representation of ~~the~~ wake characteristics under different atmospheric conditions ~~, specifically accounting for turbulence intensity,~~ and different turbine operating conditions. Good agreement was also seen with the Jensen and ~~multizone wake model~~ multi-zone wake models on a smaller subset of data that matched the conditions of the tuning data. ~~Future work will include the modeling and analysis of wake deformation and changes in veer. In addition, future wind farm control strategies will be dependent on atmospheric conditions to improve their effectiveness~~

Based on these results, this provides more confidence in wind farm controllers designed using these models. This study provided a first step towards validating these models in the field. In particular, this study focused on the wake of a single turbine. An increased understanding of these models at the wind farm level is needed to determine the potential performance of wind farm controls solutions in the field.

Acknowledgements. The Alliance for Sustainable Energy, LLC (Alliance) is the manager and operator of the National Renewable Energy Laboratory (NREL). NREL is a national laboratory of the U.S. Department of Energy, Office of Energy Efficiency and Renewable Energy. This work was authored by the Alliance and supported by the U.S. Department of Energy under Contract No. DE-AC36-08GO28308~~with the National Renewable Energy Laboratory. Funding for the work~~ . Funding was provided by the ~~DOE~~ U.S. Department of Energy Office of Energy Efficiency and Renewable Energy, Wind Energy Technologies Office. The views expressed in the article do not necessarily represent the views of the U.S. ~~Government retains~~Department of Energy or the U.S. government. The U.S. government retains, and the publisher, by accepting the article for publication, acknowledges that the U.S. ~~Government~~ government retains a nonexclusive, paid-up, irrevocable, worldwide license to publish or reproduce the published form of this work, or allow others to do so, for U.S. ~~Government~~ government purposes.

6 Appendix: FLORIS tuning values for near-wake lidar comparisons

Due to the limitations of the field data presented in this paper, FLORIS had to be tuned to capture the near-wake behind the turbine. The wake was evaluated primarily at 2.35D (180.95 m) downstream. These parameters were tuned for 5% turbulence intensity as indicated in the analysis. Below are the FLORIS tuning values for the near-wake lidar comparisons shown in this paper:

- Jensen Wake Model
  - $k_e = 0.055$
  - $k_d = 0.17$
  - For high turbulence cases (> 10% turbulence intensity), $k_e = 0.1$.
- Multi-zone Wake Model
  - $k_e = 0.1$

- $k_d = 0.17$
- $m_c = -0.5, 0.3, 1.0$
- $M_U = 0.47, 1.28, 5.5$
- $a_U = 11.7$
- $b_U = 0.72$
- For high turbulence cases (> 10% turbulence intensity), $k_e = 0.13$.

- Gaussian Wake Model
  - $k_a = 0.17$
  - $k_b = 0.06$

References

Abkar, M. and Porté-Agel, F.: Influence of atmospheric stability on wind-turbine wakes: A large-eddy simulation study, Physics of Fluids, 27, 035 104, 2015.

Annoni, J., Gebraad, P. M., Scholbrock, A. K., Fleming, P. A., and Wingerden, J.-W. v.: Analysis of axial-induction-based wind plant control using an engineering and a high-order wind plant model, Wind Energy, 2015.

Bastankhah, M. and Porté-Agel, F.: A new analytical model for wind-turbine wakes, Renewable Energy, 70, 116–123, 2014.

Bastankhah, M. and Porté-Agel, F.: Experimental and theoretical study of wind turbine wakes in yawed conditions, Journal of Fluid Mechanics, 806, 506–541, 2016.

Boersma, S., Doekemeijer, B., Gebraad, P., Fleming, P., Annoni, J., Scholbrock, A., Frederik, J., and van Wingerden, J.: A tutorial on control-oriented modeling and control of wind farms, in: Proceedings of the American Control Conference (ACC), Seattle, USA, 2017.

Burton, T., Sharpe, D., Jenkins, N., and Bossanyi, E.: Wind energy handbook, John Wiley & Sons, 2001.

Campagnolo, F., Petrović, V., Bottasso, C. L., and Croce, A.: Wind tunnel testing of wake control strategies, in: American Control Conference (ACC), 2016, pp. 513–518, IEEE, 2016.

Chamorro, L. P. and Porté-Agel, F.: Turbulent flow inside and above a wind farm: a wind-tunnel study, Energies, 4, 1916–1936, 2011.

Dilip, D. and Porté-Agel, F.: Wind Turbine Wake Mitigation through Blade Pitch Offset, Energies, 10, 757, 2017.

Fleming, P., Annoni, J., Churchfield, M., Martinez, L., Gruchalla, K., Lawson, M., and Moriarty, P.: From Wake Steering to Flow Control, Submitted to Wind Energy Science, 2017a.

Fleming, P., Annoni, J., Scholbrock, A., Quon, E., Dana, S., Schreck, S., Raach, S., Haizmann, F., and Schlipf, D.: Full-Scale Field Test of Wake Steering, in: Wake Conference, Visby, Sweden, 2017b.

Fleming, P., Annoni, J., Shah, J. J., Wang, L., Ananthan, S., Zhang, Z., Hutchings, K., Wang, P., Chen, W., and Chen, L.: Field test of wake steering at an offshore wind farm, Wind Energy Science, 2, 229, 2017c.

Fleming, P. A., Gebraad, P. M., Lee, S., van Wingerden, J.-W., Johnson, K., Churchfield, M., Michalakes, J., Spalart, P., and Moriarty, P.: Evaluating techniques for redirecting turbine wakes using SOWFA, Renewable Energy, 70, 211–218, 2014.

Fleming, P. A., Ning, A., Gebraad, P. M., and Dykes, K.: Wind plant system engineering through optimization of layout and yaw control, Wind Energy, 19, 329–344, 2016.

Gebraad, P., Teeuwisse, F., Wingerden, J., Fleming, P., Ruben, S., Marden, J., and Pao, L.: Wind plant power optimization through yaw control using a parametric model for wake effects—a CFD simulation study, Wind Energy, 19, 95–114, 2016.

Gebraad, P. M. and Van Wingerden, J.: A control-oriented dynamic model for wakes in wind plants, in: Journal of Physics: Conference Series, vol. 524, p. 012186, IOP Publishing, 2014.

Howland, M. F., Bossuyt, J., Martínez-Tossas, L. A., Meyers, J., and Meneveau, C.: Wake structure in actuator disk models of wind turbines in yaw under uniform inflow conditions, Journal of Renewable and Sustainable Energy, 8, 043 301, 2016.

Jensen, N. O.: A note on wind generator interaction, Tech. Rep. Risø-M-2411, Risø, 1983.

Jiménez, Á., Crespo, A., and Migoya, E.: Application of a LES technique to characterize the wake deflection of a wind turbine in yaw, Wind energy, 13, 559–572, 2010.

Johnson, K. E. and Thomas, N.: Wind farm control: Addressing the aerodynamic interaction among wind turbines, in: American Control Conference, pp. 2104–2109, 2009.

Johnson, K. E., Pao, L. Y., Balas, M. J., and Fingersh, L. J.: Control of variable-speed wind turbines: standard and adaptive techniques for maximizing energy capture, Control Systems, IEEE, 26, 70–81, 2006.

Jonkman, J.: NWTC Design Codes - FAST, https://nwtc.nrel.gov/FAST, 2010.

Jonkman, J. M., Butterfield, S., Musial, W., and Scott, G.: Definition of a 5-MW reference wind turbine for offshore system development, 2009.

Katic, I., Højstrup, J., and Jensen, N. O.: A simple model for cluster efficiency, in: European wind energy association conference and exhibition, pp. 407–410, 1986.

Mendoza, I., Hur, J., Thao, S., and Curtis, A.: Power performance test report for the US Department of Energy 1.5-megawatt wind turbine, Tech. rep., National Renewable Energy Laboratory (NREL), Golden, CO (United States), 2015.

Niayifar, A. and Porté-Agel, F.: A new analytical model for wind farm power prediction, in: Journal of Physics: Conference Series, vol. 625, p. 012039, IOP Publishing, 2015.

Niayifar, A. and Porté-Agel, F.: Analytical modeling of wind farms: A new approach for power prediction, Energies, 9, 741, 2016.

Pope, S. B.: Turbulent flows, Cambridge university press, 2000.

Raach, S., Schlipf, D., and Cheng, P. W.: Lidar-based wake tracking for closed-loop wind farm control, in: Journal of Physics: Conference Series, vol. 753, p. 052009, IOP Publishing, 2016.

Raach, S., Boersma, S., van Wingerden, J.-W., Schlipf, D., and Cheng, P. W.: Robust lidar-based closed-loop wake redirection for wind farm control, IFAC-PapersOnLine, 50, 4498–4503, 2017.

Roadman, J. and Huskey, A.: Acoustic Noise Test Report for the US Department of Energy 1.5-Megawatt Wind Turbine, Tech. rep., National Renewable Energy Lab.(NREL), Golden, CO (United States), 2015.

Santos, R. and van Dam, J.: Mechanical Loads Test Report for the US Department of Energy 1.5-Megawatt Wind Turbine, Tech. rep., National Renewable Energy Laboratory (NREL), Golden, CO (United States), 2015.

Schottler, J., Hölling, A., Peinke, J., and Hölling, M.: Wind tunnel tests on controllable model wind turbines in yaw, in: 34th Wind Energy Symposium, vol. 1523, 2016.

Smalikho, I., Banakh, V., Pichugina, Y., Brewer, W., Banta, R., Lundquist, J., and Kelley, N.: Lidar investigation of atmosphere effect on a wind turbine wake, Journal of Atmospheric and Oceanic Technology, 30, 2554–2570, 2013.

Stanley, A. P., Thomas, J., Ning, A., Annoni, J., Dykes, K., and Fleming, P.: Gradient-Based Optimization of Wind Farms with Different Turbine Heights, in: 35th Wind Energy Symposium, p. 1619, 2017.

Stull, R. B.: An introduction to boundary layer meteorology, vol. 13, Springer Science & Business Media, 2012.

Thomas, J., Tingey, E., and Ning, A.: Comparison of two wake models for use in gradient-based wind farm layout optimization, in: Technologies for Sustainability (SusTech), 2015 IEEE Conference on, pp. 203–208, IEEE, 2015.

Vollmer, L., Steinfeld, G., Heinemann, D., and Kühn, M.: Estimating the wake deflection downstream of a wind turbine in different atmospheric stabilities: an LES study, Wind Energy Science, 1, 129–141, 2016.